

STUDY OF CONTACTS IN AN ELECTROSTATICALLY ACTUATED MICROSWITCH

Sumit Majumder¹, N. E. McGruer, George G. Adams, P. M. Zavracky, Richard H. Morrison, and
Jacqueline Krim
Northeastern University
360 Huntington Avenue
Boston, MA 02115

Abstract

Surface micromachined, electrostatically actuated microswitches have been developed at Northeastern University. Microswitches with gold contacts typically have an initial contact resistance of the order of 0.1Ω over the first 10^5 cycles of lifetime while cold-switching 4 mA, and have a current handling capability of about 20 mA. In general, the contact resistance decreases over the first few thousand switch cycles, and degrades progressively when the switches are cycled beyond approximately 10^6 cycles. In this work, the microswitch contact resistance is studied on the basis of a clean metal contact resistance model. Comparison of the measured contact resistance (measured as a function of contact force) with the characteristics predicted by the model shows approximate agreement. The discrepancies between the model characteristics and measurements are discussed briefly.

Keywords: microswitches; contact resistance.

I. Introduction

Electrostatically actuated micromechanical switches have been developed at Northeastern University, using a simple microfabrication process [1]. Figure 1 is a schematic representation of a microswitch, and Figure 2 shows an SEM micrograph of a fabricated device. In its simplest form, the microswitch is based on a double cantilever beam, and has 3 electrical terminals, labeled source, gate and drain in Figures 1 and 2. Applying a voltage between the gate and source terminals creates an electrostatic force between the gate electrode and the cantilever, and pulls the beam down to create electrical contact between the drain and source terminals.

¹ Corresponding author. Fax: +1 617 373 7878, e-mail: sumit@ece.neu.edu, phone: +1 617 373 3518, address: Dept. of Electrical and Computer Engineering, 409 Dana Research Building, Northeastern University, 360 Huntington Ave, Boston, MA 02115, USA.

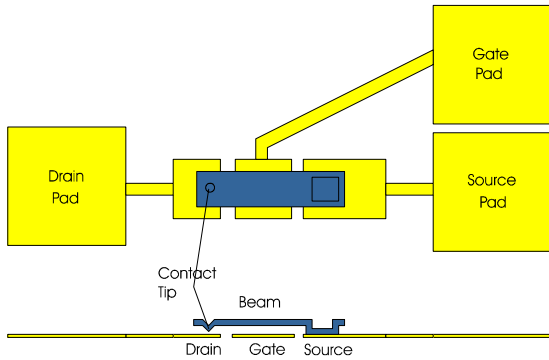


Figure 1 Schematic of a microswitch. Application of a voltage between the gate and source electrodes pulls the cantilever beam down and closes the microswitch.

When the microswitch closes, contact between the beam and the drain electrode occurs through a pair of bumps on the lower surface of the beam, near its free end. Figure 3 shows a detailed view of a contact bump on the bottom of a beam that was flipped over with a probe.

Analysis and measurement of the performance of our microswitches has been reported earlier in [2] and [3]. The minimum actuating gate-to-source voltage required to close a microswitch is typically 20-60 V, depending on the device geometry. This is referred to as the threshold voltage in this paper.

Switches have been tested while being cycled in excess of 10^8 cycles. Testing is done in a nitrogen ambient, at atmospheric pressure, with current being applied to the contacts during each cycle only when the switch is in a closed position. The current through the switch is between 4 mA and 20 mA. Switches with gold-on-gold contacts typically have an initial contact resistance between 0.5 - 5 Ω . Cycling the switches results in a reduction in the contact resistance over the first 10^4 - 10^5 switching cycles, to less than 0.1 Ω (Figure 4). Beyond 10^5 - 10^7 cycles,

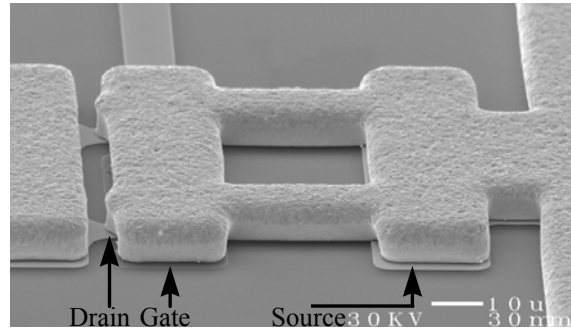


Figure 2 SEM micrograph of a microswitch (the scale bar corresponds to 10 microns). The fixed end of the double cantilever beam is on the right. The source, gate and drain electrodes (from right to left) are visible underneath the beam.

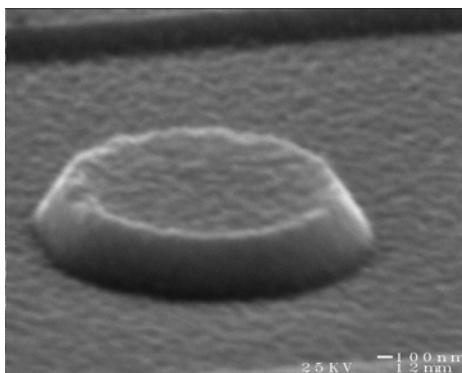


Figure 3 SEM micrograph showing close-up of a contact bump on a microswitch that was flipped over.

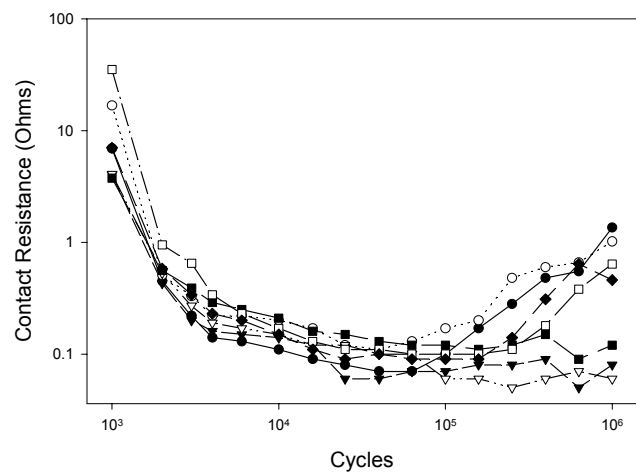


Figure 4 Variation in contact resistance over first 10^6 switching cycles of 7 switches belonging to a single die.

contact resistance is typically found to increase progressively. Switches eventually fail in one of two modes - they either stay closed permanently, or their resistance increases progressively as they are cycled.

Microswitches with 2 contact bumps usually have a shortened lifetime if the current through the microswitch exceeds 20mA. Current handling capability in excess of 150 mA has been obtained with switches with a larger number of contacts.

In this paper, we present recent work on the modeling and measurement of the microswitch contact resistance. We first describe a simple, clean-metal contact resistance model. We then present contact resistance measurement data and compare experimental results with the model.

II. Contact Resistance Model

Modeling of the contact resistance can be broadly divided into 3 successive steps: determining the contact force as a function of the applied gate voltage; determining the distribution and sizes of the areas in contact at the contact interface, as a function of the contact force; and determining the contact resistance as a function of the distribution and sizes of the areas in contact (this approach follows in part the modeling discussed by Beale and Pease in [4]). Based on this approach, a contact resistance model is discussed in this section.

Contact Force

The contact force can be determined as a function of the gate voltage by modeling the microswitch as a beam which is clamped at its fixed end, and simply supported at its free end. The Euler-Bernoulli beam equations are used to determine the beam deflection and contact force boundary condition, assuming a certain distributed electrostatic force acting on the beam. In turn, the new electrostatic force is determined as a function of the beam shape. The two

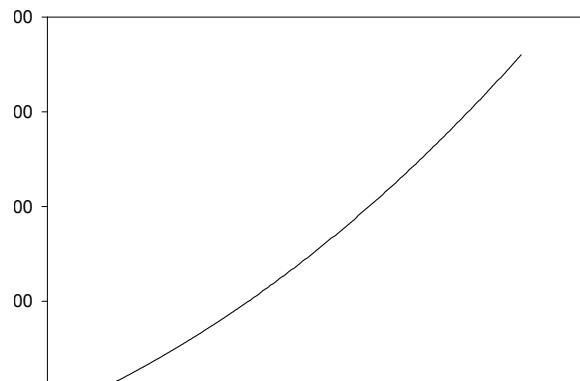


Figure 5 Modeled variation of contact force with gate voltage for a typical microswitch geometry.

steps are repeated iteratively, until the solution converges. A more detailed description is given in [5], and a similar procedure for determining the threshold voltage is described in [2]. Figure 5 shows the modeled variation of contact force with gate voltage for a typical microswitch geometry.

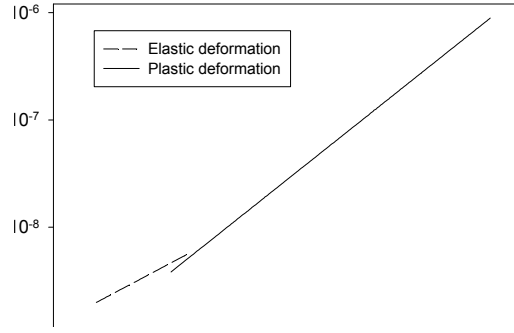
Contact Area

Determining the nature of the contact area at the interface necessitates a model of the surface profiles of the contact bump and the drain electrode. In the switches considered in this discussion, the contact is gold-on-gold. SEM micrographs of the contact bump surface, and SEM micrographs and STM scans of the drain electrode surface indicate that the contact bump is significantly rougher than the drain electrode. The drain electrode is assumed, therefore, to be a flat surface. The SEM micrograph of a contact bump shown in Figure 3 suggests that the contacting asperities on the surface of the contact bumps have tip radii of 50-200 nm, and that a few asperities, or at most tens of asperities, will make contact. A rigorous modeling of the surface profile of the contact would require an accurate surface profile of the contact bump. However, it is instructive to study the contact resistance characteristics on the basis of some simple surface profile models. Accordingly, we consider 3 different surface profiles: profile A consists of a single spherical asperity with of radius 100 nm; profile B consists of 5 identical asperities of radius 100 nm, whose heights vary over a range of 80nm; profile C consists of 50 identical asperities of radius 100 nm, with heights varying over a range of 80nm. It has been reported in the literature that thin films, in general, have higher values of hardness than the corresponding bulk material. We use a value of 2 GPa for the hardness of gold, as reported in [6].

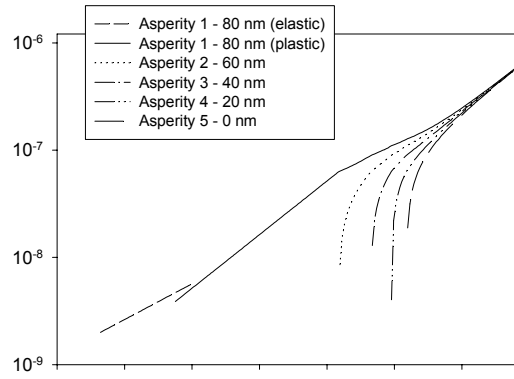
Contact between the contact bump and the drain is modeled as follows. When the contact bump is pressed against the surface of the drain electrode with a certain contact force, the asperities on the contact bump deform, forming circular contact spots. The number of contact spots and their sizes can be determined on the basis of the elastic-plastic model for contact of a rough surface with a flat plane, proposed by Chang, Etsion and Bogy [7]. This model is a refinement of the well-known "asperity based model" introduced by Greenwood and Williamson [8], in which the rough surface is represented by a collection of spherical asperities with identical end radii, whose heights have a statistical distribution. The asperities are assumed to be independent of each other, that is, the load on one asperity does not affect the deformation of another. The area of contact for each asperity in the Greenwood-Williamson model is calculated from the Hertz theory of elastic deformation, even though at a particular contact force the loads on some of the asperities may have exceeded the elastic limit so that the asperities deform plastically. The model proposed by Chang, et al. calculates the deformation of a plastically deformed asperity on the basis of volume conservation of a certain control volume of the asperity. In the following paragraphs, we briefly explain the equations governing the above model.

Let the moduli of elasticity of the contacting surfaces be denoted by E_1 and E_2 , respectively, and their Poisson's ratios by ν_1 and ν_2 respectively. The effective modulus of elasticity is defined as

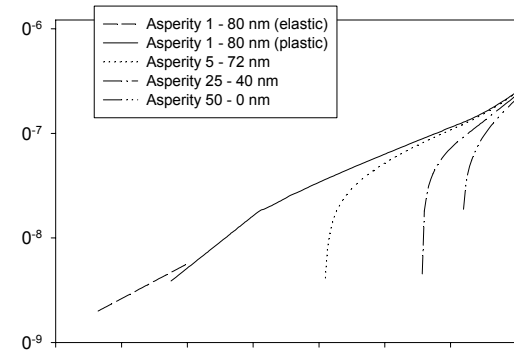
$$\frac{1}{E'} = \frac{1-\nu_1^2}{E_1} + \frac{1-\nu_2^2}{E_2}. \quad (1)$$



(6a)



(6b)



(6c)

Figure 6 Modeled variation of contact radii with contact force for the single asperity of surface profile A (6a), for each of the 5 asperities of surface profile B (6b), and for 4 of the 50 asperities of surface profile C (6c).

For an elastically deformed asperity, the radius of the contact spot, r , is related to the force on the asperity, F , as

$$r = \left(\frac{3FR_t}{4E'} \right)^{1/3}, \quad (2)$$

where R_t denotes the end radius of curvature of the asperity. Also, the contact radius r is related to the vertical deformation of the asperity, α , as

$$r = \sqrt{R_t \alpha}. \quad (3)$$

The onset of plastic yielding is assumed to occur when the maximum pressure at the contact interface exceeds $0.6 H$, where H is hardness of the contacting material. The vertical deformation of the asperity at this point is given by

$$\alpha_c = \left(\frac{0.3\pi H}{E} \right)^2 R_t. \quad (4)$$

In the plastic region, the average pressure on an asperity is assumed to be $0.6 H$, so that the contact force on the asperity is

$$F = 0.6\pi H r^2. \quad (5)$$

The contact radius is determined in terms of the vertical deformation α by invoking conservation of volume of the deformed asperity:

$$r = \sqrt{R_t \alpha \left(2 - \frac{\alpha_c}{\alpha} \right)}, \quad \alpha > \alpha_c. \quad (6)$$

Hence, for a given vertical deformation, the force on each asperity as well as the radius of the corresponding contact spot can be determined.

Now consider a rough surface with N asperities, each with an end radius of curvature R_t , and heights $z_1 > z_2 > \dots > z_N$. Let the separation between the reference planes be d for a given contact force F , such that $z_n > d > z_{n+1}$. Then asperities $1, 2, \dots, n$ come into contact. The vertical deformation of asperity i is given by

$$\alpha_i = z_i - d. \quad (7)$$

For a given separation between the reference planes, the force on each asperity, and the radius of each of the corresponding contact spots can be obtained using the previously stated equations. Figure 6 shows the variation of contact radii with the contact force for the single asperity of surface profile A, for all the asperities of surface profile B, and for 4 of the 50 asperities of surface profile C. The discontinuity occurring at approximately 10^{-7} N in the characteristic of Figure 6a, and in the characteristic corresponding to the tallest asperity in 6b and 6c, corresponds to the transition region from elastic to plastic deformation. Each of the shorter asperities too deforms elastically when it first comes into contact, but the discontinuity in the transition from elastic to plastic deformation is not visible on a logarithmic force scale.

Contact Resistance

The remaining step is to determine the contact resistance, given a certain number of contact spots of known radii. We first consider the contact resistance of a single spot of a given radius r , separating 2 semi-infinite bodies of resistivity ρ . If the radius r is small compared to the electron mean free path length l_e of the material, the resistance of the contact spot is dominated by the Sharvin mechanism [9], in which electrons are projected ballistically through the contact spot without being scattered. In this case,

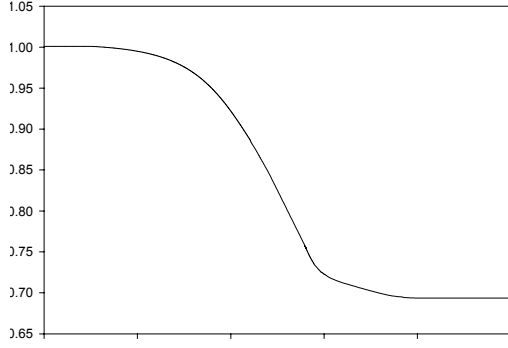


Figure 7 Variation of the interpolation parameter ν (used in equation 10) with the Knudsen ratio l_e/r

$$R = \frac{4\rho l_e}{3\pi r^2} \quad (8)$$

On the other hand, if the radius is much larger than the mean free path length, the resistance is dominated a diffuse scattering mechanism, and is given by the Maxwell spreading resistance formula[10]:

$$R = \frac{\rho}{2r} \quad (9)$$

Wexler [11] has given a solution of the Boltzmann equation, using the variational principle for resistance of a circular contact spot separating semi-infinite bodies. This results in a simple interpolation formula which can account for the transition between the Maxwell and Sharvin regimes.

$$R = \frac{4\rho l_e}{3\pi r^2} + \nu(l_e/r) \frac{\rho}{2r} \quad (10)$$

ν is a slowly varying function of the ratio l_e/r (Figure 7), with $\nu(0)=1$, and $\nu(\infty)=0.694$.

In general, multiple asperities come into contact, resulting in multiple contact spots of varying sizes. The effective contact resistance arising from the contact spots depends on the radii of the spots (given by the contact area model discussed previously) and the distribution of the spots on the contact surface. A lower bound can be obtained on the contact resistance by assuming that contact spots are independent and conduct in parallel (this is equivalent to the exact solution when the radii of the contact spots are small compared to the separation between the spots). Denoting the contact resistance of spot i as R_i ,

$$1/R_{lb} = \sum_i 1/R_i \quad (11)$$

An upper bound can be obtained on the contact resistance by computing the resistance of a circular spot of radius r_{eff} , and of area equal to the total area of all the individual contact spots combined. This upper bound is equivalent to the exact solution when all the conducting spots become large enough to merge into a single conducting spot.

$$R = \frac{4\rho l_e}{3\pi r_{eff}^2} + \nu(l_e/r) \frac{\rho}{2r_{eff}} \quad (12)$$

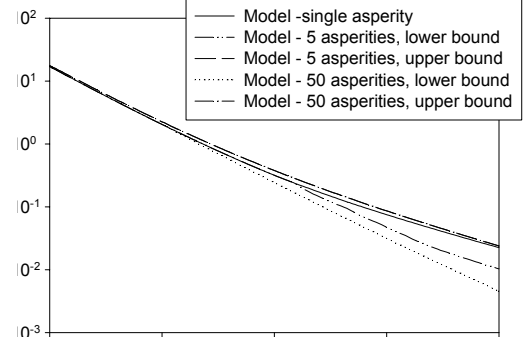


Figure 8 Modeled contact resistance vs contact force characteristics.

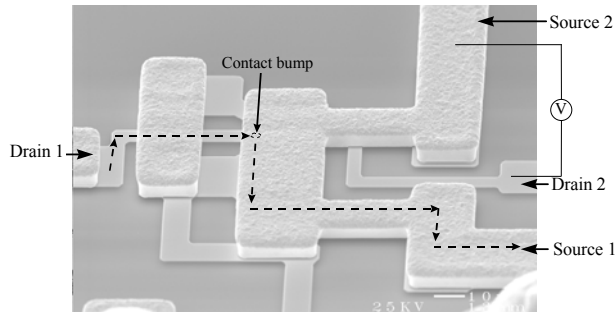


Figure 9 Microswitch geometry used to measure contact resistance. Current (represented by the broken lines) is forced between one pair of source and drain terminals, and the other pair of source and drain terminals is used to measure the voltage across the contact. The contact bump on the lower surface of the beam is not visible in this micrograph.

Radius of contact spot	0.1 μm	0.5 μm	1 μm
$R = \frac{\rho}{2r}$	0.11 Ω	0.02 Ω	0.01 Ω
Resistance from finite element	0.11 Ω	0.021 Ω	0.013 Ω

Table 1 Comparison of contact resistance obtained by a Poisson's equation finite element simulation of the microswitch contact geometry shown in Figure 9, with the Maxwell model contact resistance of an idealized geometry consisting of 2 semi-infinite contact bodies separated by a circular contact spot.

With the models described above, it is possible to determine the upper and lower bounds of contact resistance as a function of the contact force. Figure 8 shows the variation of contact resistance with contact force for the surface profiles A, B, and C. All the contact resistance characteristics are identical at a low contact force, when only a single asperity is in contact. The bounds become progressively looser as the resistance decreases, and as the number of asperities in contact increases. Figure 9 also shows measured contact resistance characteristics for comparison. These are discussed in the next section.

III. Measurements

Contact resistance was measured using a modification of the microswitch geometry described earlier. The microswitch structure used to measure contact resistance (shown in Figure 9) has an extra pair of terminals which allow the voltage across the contact to be measured. The question arises whether the idealization of semi-infinite contact members is applicable to the microswitch geometry, since the beam is 5-7 microns thick, and the contact pad on the substrate is only 0.2 micron in thickness. A finite element program solving Poisson's equation was used to simulate the contact resistance of the switch geometry of Figure 9, assuming a single contact spot of a certain radius. Table 1 shows the contact resistance given by the finite element simulation, compared with the Maxwell contact resistance for the corresponding idealized geometry. The idealization appears to be quite reasonable over the range of contact radii of interest.

The contact resistance measurement was carried out in a nitrogen ambient, with a current of 4 mA passing through the contact. Figure 10a) shows the initial contact resistance of a group of nine microswitches, measured while the gate-to-source voltage was increased in steps. There is a substantial variation in measured contact resistance over the group, approximately between 70 m Ω and 10 Ω . As mentioned earlier and seen in Figure 4, the microswitch contact resistance generally decreases from the initial value as the switch is cycled. Figure 10b) shows the contact resistance characteristics of the same group of switches as in 10a), after they have been cycled 300 times. Most of the switches now have a significantly smaller contact resistance - the decrease in resistance with the

number of switching cycles is evidently more abrupt than seen in Figure 4, possibly because these switches were subject to a higher contact force. The sample-to-sample variation in contact resistance is also much smaller than in 10a), with the contact resistance of 7 of the 9 switches varying between approximately 30 m Ω and 70 m Ω . The predicted contact resistance versus force characteristics from Figure 9 are re-plotted in Figures 10a) and 10b) for comparison. The contact resistance characteristics during the first switch cycle, shown in Figure 10b), are in most cases 1-2 orders of magnitude higher than the predicted characteristics. The decrease in contact resistance as switches are cycled suggests that much of this discrepancy is due to an initial insulating film at the interface. Comparison of the measured contact resistance characteristics after 300 switch cycles (Figure 10b) with the model shows that at small contact forces, the measured contact resistance is significantly smaller and less sensitive to the contact force than the model predicts; there is better agreement between the measured and predicted characteristics at higher contact forces. This may be partly explained by the fact that the contact surfaces deform plastically, so that the contact area defined by plastic deformation during a switch cycle determines the contact resistance at small contact forces during the next switch cycle.

It should also be noted that adhesive forces at the contact interface have not been taken into account in the model, and there is some evidence that these forces may be significant. The turn-off voltage (the gate-to-source voltage at which a microswitch just turns off) was measured for a group of devices, at periodic intervals as they were cycled. The contact resistance of the microswitches was also measured at the same intervals. Figure 11 shows the turn-off voltage plotted as a function of the contact resistance (the variation of contact resistance with switch cycles for the same group of switches is seen in Figure 4). When the contact resistance is relatively high, the microswitches turn off at nearly the same voltage at which they turn on (55 - 60 V). However, when the contact resistance is small - in the relatively stable portion of the resistance versus lifetime characteristics of Figure 4 - the turn-off voltage is much smaller - 20-30 V - indicating the existence of adhesive forces which tend to hold the switches closed. It is well known that electrostatically actuated cantilevers are electromechanically hysteretic - the voltage required to pull the cantilever down to a closed position is higher than the voltage at which it opens [1]. However, the variability of the turn-off voltage indicates that this effect is not responsible for the observed hysteresis. Modeling of the turn-off voltage, using the Euler-Bernoulli beam model used to calculate the contact force [5], and modeling of the threshold voltage using the same beam equations [2], predicts a difference of less than 2V between threshold and turn-off voltage for typical switch dimensions.

There are other possible sources of deviation of the measured characteristics from the model. The initial decrease in contact resistance as the switch is cycled (Figure 4) suggests the possibility of insulating films existing at the contact interface, at least initially. Also, the hardness of the contact surfaces is assumed to be 2 GPa in the model, and is not experimentally determined. If the actual hardness is significantly different, this would be partly responsible for discrepancy between the measurement and the model.

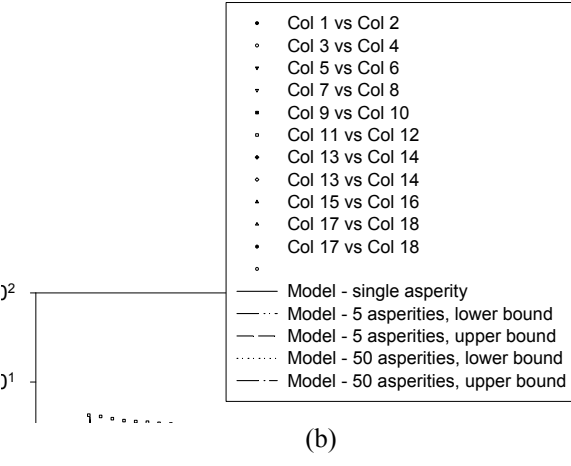
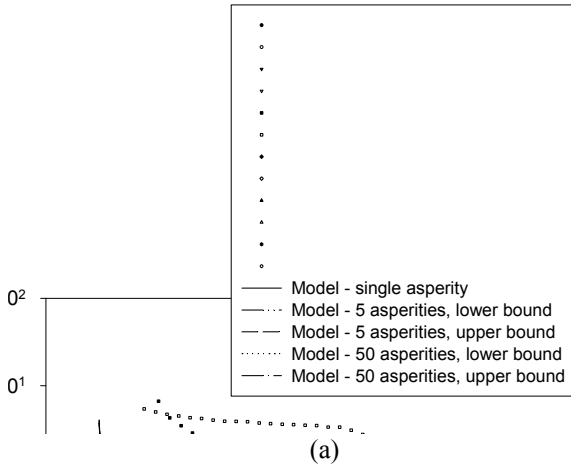


Figure 10 Measured contact resistance characteristics of a group of 9 switches belonging to a single die, with modeled characteristics shown on the same graph for comparison: a) initial contact resistance; b) contact resistance after 300 switch cycles.

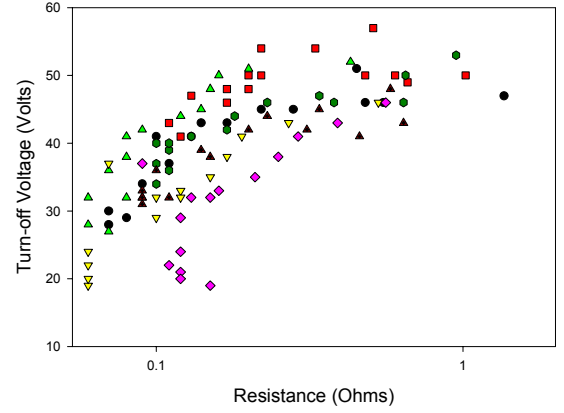


Figure 11 Measured turn-off voltage of a group of 7 microswitches; each device was cycled 10^6 times, and its contact resistance and turn-off voltage was measured at intervals while cycling. The measured turn-off voltage is plotted as a function of contact resistance (Figure 4 shows the contact resistance plotted as a function of switch cycles for the same group of microswitches).

IV. Conclusions

Contact resistance characteristics of an electrostatically actuated microswitch have been studied on the basis of a clean-metal model. An initial, gradual decrease in the contact resistance is observed as the switch is cycled, possibly due to insulating films at the contact interface.. The measured contact resistance after this initial decrease has fairly good agreement with the modeled characteristics. At low contact forces, the measured contact resistance is smaller and less sensitive to the contact force than is predicted by the model. Factors contributing to this discrepancy may include plastic deformation of the contact surfaces during earlier switch cycles, and adhesive forces at the contact interface. The existence of adhesive forces is supported by measurements showing that when the contact resistance is low, the turn-off voltage is much smaller than the threshold voltage of the switch. The surface hardness value

used in the model has not been verified experimentally, and this too may contribute to some of the observed discrepancy.

V. Acknowledgments

This work was funded by Analog Devices. We would like to acknowledge the contributions of Weilin Hu of Northeastern University, and would like to thank Dave Potter, Mark Schirmer and Curtis Davis of Analog Devices for their contributions, advice and support.

References

- [1] P.M. Zavracky, N.E. McGruer, and S. Majumder, "Micromechanical Switches Fabricated using Nickel Surface Micromachining", *Journal of Microelectromechanical Systems*, **6**, 3-9 (1997).
- [2] S. Majumder, P.M. Zavracky, N.E. McGruer, "Electrostatically Actuated Micromechanical Switches", *Journal of Vacuum Science and Technology B*, **15**, 1246, (1997).
- [3] S. Majumder, N. E. McGruer, P.M. Zavracky, G. G. Adams, R. H. Morrison, J. Krim, "Measurement And Modeling Of Surface Micromachined, Electrostatically Actuated Microswitches", *Transducers '97*, Chicago, IL (1997).
- [4] J. P. Beale and R.F.W. Pease, "Apparatus for Studying Ultrasmall Contacts", *Proceedings of the 38th IEEE Holm Conference on Electrical Contacts*, Philadelphia, PA (1992).
- [5] S. Majumder, "Electrostatically Actuated Micromechanical Switches", Master's Thesis, Northeastern University, Boston, MA (1996).
- [6] W. C. Oliver, R. Hutchings, and J.B. Pethica, "Measurement of Hardness at Indentation Depths as Low as 20 nanometers", in *Microindentation Techniques in Materials Science and Engineering*, ASTM STP 889, Philadelphia, 90-108 (1986).
- [7] W. R. Chang, I. Etsion, and D.B. Bogy, "An Elastic-Plastic Model for the Contact of Rough Surfaces", *Journal of Tribology*, **109**, 257-263. (1988).
- [8] J. A. Greenwood, and J.B.P. Williamson, "Contact of Nominally Flat Surfaces", *Proceedings of the Royal Society (London)*, **A295**, 300-319. (1966).
- [9] A. G. M. Jansen, A. P. van Gelder, and P. Wyder, "Point-Contact Spectroscopy in Metals", *Journal of Physics*, **C13**, 6073-6118. (1980).
- [10] R. Holm, *Electric Contacts*, Springer-Verlag (New York), 1967.
- [11] G. Wexler, "The Size Effect and the Non-Local Boltzmann Transport Equation in Orifice and Disk Geometry", *Proceedings of Physical Society*, **89**, 927-941. (1966)